APPENDIX

Mass Transfer and Concentration Polarization in Rotating Reverse Osmosis

Sangho Lee and Richard M. Lueptow[*]

Department of Mechanical Engineering, Northwestern University, Evanston, IL, 60208, U.S.A.

Keywords: Reverse Osmosis; Rotating Filtration; Concentration Polarization; Mass Transfer

Concentration polarization and subsequent membrane fouling are serious obstacles that limit the acceptance of Reverse Osmosis (RO) membrane treatment. Therefore, the reduction and alleviation of concentration polarization in filtration and RO have been the focus of much research and development (Matthiasson and Sivik, 1980). Recently, rotating filtration has been proposed for RO to minimize concentration polarization (Lee and Lueptow, 2001). A rotating filter, which consists of a cylindrical filter rotating within a stationary cylindrical shell, takes advantage of centrifugal flow instabilities to reduce the plugging of the filter pores during microfiltration and ultrafiltration (Holeschovsky and Cooney, 1991; Belfort et al., 1993). A similar reduction in concentration polarization is expected to occur for rotating RO (Lee and Lueptow, 2001).

At low rotational speeds the flow in the annulus between a rotating inner cylinder and a fixed outer cylinder has a nearly linear azimuthal velocity profile and no other remarkable features. However, the flow becomes unstable having toroidal vortical cells known as Taylor vortices stacked in the annulus above a particular dimensionless rotational speed, $Re(d/r_i)^{1/2}$, where $Re = r_i\omega d/\nu$ is the rotating Reynolds number, r_i is the inner cylinder radius, ω is the rotational speed, d is the gap between the inner and outer cylinders, and ν is the kinematic viscosity. These vortices, which become stronger with increasing Re, cause a redistribution of the azimuthal momentum in the annulus resulting in a steep velocity gradient at the inner cylinder (Wereley and Lueptow, 1994; Akonour and Lueptow, 20012). In the cases of microfiltration of a suspension at a porous inner cylinder or mass transfer of a chemical species in a cylindrical chemical reactor with a non-porous inner cylinder, experiments have shown that this higher shear results in an increased mass transfer when the flow changes from non-vortical to vortical. Furthermore, the mass transfer is enhanced with increasing Re as the vortices grow in strength.

Although several studies have been performed to obtain mass transfer correlations in vortical flow devices for transport of a suspension in a rotating cylindrical filter device and for transport of a solute in a cylindrical chemical reactor with a non-porous inner cylinder, no measurements have been made for rotating RO membrane filtration

[*] Corresponding author

systems where solute concentration polarization at a porous inner cylinder is of concern. In this study, we measure the mass transfer coefficient in a rotating RO system and its dependence on the rotating Reynolds number. The mass transfer coefficient measured in this study will be of use in analytical models of rotating RO (Lee and Lueptow, 2001)

Theoretical Background

The solvent flux, J_v, through the inner cylinder membrane is:

$$J_v = L_v \left(\Delta P - P_{loss} \right) \tag{1}$$

where L_v is the solvent transport parameter, ΔP is the pressure difference from the device inlet to the permeate side of the membrane, and $P_{loss} = \Delta \Pi + \Delta P_h$ is the pressure loss by osmotic pressure, $\Delta \Pi$, and hydrodynamic effects in the annulus, ΔP_h. The osmotic pressure can be calculated by Van't Hoff's equation (Snoeyink and Jenkins, 1980):

$$\Delta \Pi = \left(C_m - C_p \right) RT \tag{2}$$

where C_m and C_p are the solute concentrations at the membrane surface on the concentrate side and the permeate side of the membrane, R is the gas constant, and T is temperature. For the conditions considered here, ΔP_h is negligible compared to $\Delta \Pi$.

The solute concentration at the membrane, C_m, can be estimated from the pressure difference, the permeate concentration, and the water flux, by rearranging Eqn (1) and (2):

$$C_m = \frac{1}{RT} \left(\Delta P - \frac{J_v}{L_v} \right) + C_p \tag{3}$$

On the basis of the film model theory and from Fick's law for diffusion, the concentration profile near the membrane surface is:

$$\frac{C_m - C_p}{C_b - C_p} = e^{\frac{J_v}{k}} \tag{4}$$

where C_b is the solute concentration in bulk (concentrate) solution and k is the mass transfer coefficient for the back diffusion of the solute from the membrane to the bulk solution on high pressure side of membrane (Zeman and Zydney, 1996). Rearranging Eqn (4) using Eqn (3) provides an expression for the mass transfer coefficient:

$$k = \frac{J_v}{\ln\left[\frac{1}{RT}\left(\Delta P - \frac{J_v}{L_v}\right)\bigg/(C_b - C_p)\right]} \qquad (5)$$

Thus, it is relatively easy to measure the mass transfer coefficient based on a relatively simple experiment where the permeate flux, applied pressure difference, bulk solute concentration, and permeate concentration are measured. The concentration polarization ratio $f=C_m/C_b$ is then readily calculated as:

$$f = \frac{1}{C_b}\left[(C_b - C_p)e^{\frac{J_v}{k}} + C_p\right] \qquad (6)$$

Experimental Set-Up and Equipment

The test system shown in Figure 1 was used to measure the mass transfer properties for rotating RO. The rotating RO module consisted of a RO membrane rotating within an outer cylindrical housing. A commercially available thin film polymeric RO membrane (Hydranautics, U.S.A.) having water permeability of 1.61×10^{-11} m^2-sec/kg was bonded to a porous plastic cylindrical support that was mounted on a hollow steel shaft. The filter outer radius was 2.41 cm, and the inner diameter of the outer cylinder was 2.88 cm. The length of the filter surface was 12.70 cm, and the overall length of the filter chamber was 23.2 cm. A DC motor was used to rotate the inner cylindrical RO membrane at rotational speeds from 1 to 178 rpm. O-rings and shaft seals were used to seal the system under high pressure.

The input solution from a pressurized feed tank entered the annulus between the rotating RO membrane and the outer cylinder at one end of the rotating RO module and passed axially along the annulus. The permeate flowed through the rotating RO membrane, passed to the center of the hollow shaft through channels within the rotating cylindrical RO membrane unit, and exited the RO module through passageways in the endcap. After priming the test cell and flow circuit with pure water, feed solution from the pressurized reservoir was introduced into the test cell. Experiments were performed in "dynamic dead-end filtration" mode where all of the fluid entering the device passed through the RO membrane with the solute concentration building up in the annulus of the RO module. The permeate flux was measured using a graduated cylinder. After each experimental trial, all of the concentrate in the membrane module was removed to measure the final solute concentration. The viscosity and density were corrected for temperature, which varied less than 1 °C during the experiment. Two different solution were used: 4000 mg/L of

NaCl and 4000 mg/L of Na_2SO_4. Solute concentrations were measured using a conductivity meter and spectrophotometric methods (Hach, 1992).

Results and Discussion

The experimental and theoretical results in the literature for measurements of the mass transfer coefficient for filtration of suspensions in a cylindrical porous rotating cell or the transport of a chemical species in a cylindrical chemical reactor with a nonporous inner cylinder satisfy the relation:

$$Sh = A\left[Re(d/r_i)^{1/2}\right]^a Sc^b \tag{7}$$

$Sh = 2kd/D$ is the dimensionless mass transfer rate (Sherwood number), $Sc = v/D$ is the Schmidt number, and D is the diffusion coefficient of the solute (Holeschovsky and Cooney, 1991; Baier, 1999). Most previous studies of mass transfer for rotating systems conclude that A=0.4~1.1, and a=0.4~0.7 under vortical flow conditions. Using the analogy between heat and mass transfer, the exponent b for the Schmidt number is assumed to be 1/3, which has been experimentally confirmed for a large range of Schmidt numbers (Holeschovsky and Cooney, 1991; Mizushina, 1971).

In this study, 40 experimental trials, each done in triplicate, were conducted for various transmembrane pressures and rotational speeds. The mass transfer coefficients were calculated by substituting the measured flux and solute concentrations in the concentrate and the permeate into Eqn (5). Figure 2 shows the dependence of the experimentally-measured mass transfer coefficient, represented as $Sh/Sc^{1/3}$, on Reynolds number. The Sherwood number increases with Reynolds number as the rotational shear increases. In addition, the Sherwood number jumps to a higher value at the transition from non-vortical to vortical flow as the vortices redistribute azimuthal momentum leading to a higher shear. The thick solid lines through the data indicate the least squares fit for each flow regime corresponding to the following equations:

$$Sh = 2.15\left[Re(d/r_i)^{1/2}\right]^{0.18} Sc^{1/3} \quad \text{for non-vortical flow} \tag{8}$$

$$Sh = 1.05\left[Re(d/r_i)^{1/2}\right]^{0.51} Sc^{1/3} \quad \text{for vortical flow}$$

Figure 2 also compares our results with previous studies using various methods including electrochemical methods for non-porous inner cylinders (Mizushina, 1971; Coeuret and Legrand, 1981; Kataoka et al., 1977), an ultrafiltration system (Holeschovsky and Cooney, 1991), helical-tube analogy (Kawase and Ulbrecht, 1988), and a

theoretical model based on the boundary layer theory (Baier, 1999). The Sherwood numbers measured for rotating RO are slightly higher than other studies under somewhat different conditions, although the trend is consistent with previous measurements.

Using Eqn (6), contours of constant concentration polarization ratio f can be evaluated as functions of the rotational speed and transmembrane pressure. The curves shown in Figure 3 were obtained by interpolating the data from the experiments for NaCl. As expected, the smallest concentration polarization occurs at high rotational speeds and low transmembrane pressures (corresponding to low permeate flux). However, the concentration polarization decreases sharply at ω =11.7 rpm because of the flow transition from non-vortical to vortical flow. The concentration polarization decreases somewhat with rotational speed as the higher rotational shear and vortical motion prevent the build-up of rejected species at the membrane surface.

Conclusion

Mass transfer and concentration polarization in rotating RO were experimentally investigated based on film theory. The mass transfer increases having increasing rotational speed with a large positive jump at the transition from non-vortical to vortical flow, suggesting that a rotational speed sufficient to generate vortical flow in the annulus is essential to minimize concentration polarization. The mass transfer coefficients for rotating RO are slightly higher than those for other devices with similar geometries.

Notation

d = gap width, m

D = Diffusivity of solute, m^2/s

C_b = bulk concentration of solute in the annulus, g/L

C_p = solute concentration in the permeate, g/L

C_m = solute concentrate at the membrane surface, g/L

f = ratio of concentration polarization, C_w/C_b

J_v = solvent flux through the membrane, m/s

k = mass transfer coefficient, m/s

L_v = solvent transport parameter, m/s-Pa

r_i = inner cylinder radius, m

R = gas constant, 8.314 J/mole-K

T = temperature, K

ΔP = pressure difference from the device inlet to the permeate side of the membrane, Pa

$\Delta\Pi$ = osmotic pressure, Pa

ν = kinematic viscosity, m^2/s

ω = rotational speed, rad/s or rpm

Literature Cited

Akonour, A., and Lueptow, R. M. (2001). "Three-dimensional velocity field for non-wavy Taylor Couette flow." *Submitted to Journal of Fluid Mechanics.*

Baier, G. (1999). "Liquid-liquid extraction based on a new flow pattern: two fluid Taylor-Couette flow computational fluid dynamics," PhD.Thesis, University of Wisconsin, USA.

Belfort, G., Pimbley, J. M., Greiner, A., and Chung, K. Y. (1993). "Diagnosis of membrane fouling using a rotating annular filter. 1. Cell culture media." *Journal of Membrane Science*, 77, 1-22.

Coeuret, F., and Legrand, J. (1981). "Mass transfer at the electrodes of concentric cylindrical reactors combining axial flow and rotation of the inner cylinder." *Elecrochimica Acta*, 26(7), 865-872.

Hach. (1992). *Hach Water Analysis Handbook*, Hach Company, Colorado, USA.

Holeschovsky, U. B., and Cooney, C. L. (1991). "Quantitative description of ultrafiltration in a rotating filtration device." *AIChE Journal*, 37(8), 1219-1226.

Kataoka, K., Doi, H., and Komai, T. (1977). "Heat/mass transfer in Taylor vortex flow with constant axial flow rates." *International Journal of Heat and Mass Transfer*, 20, 57-67.

Kawase, Y., and Ulbrecht, J. J. (1988). "Laminar mass transfer between concentric rotating cylinders in the presence of Taylor vortices." *Electrochimica Acta*, 33(2), 199-203.

Lee, S., and Lueptow, R. M. (2001). "Rotating reverse osmosis filtration: dynamic model for flux and rejection." *Journal of Membrane Science*, 192, 129-143.

Matthiasson, E., and Sivik, B. (1980). "Concentration polarization and fouling." *Desalination*, 35, 59-103.

Mizushina, T. (1971). "The electrochemical method in transport phenomena." *Advanced Heat Transfer*, 7, 87-100.

Snoeyink, V. L., and Jenkins, D. (1980). *Water Chemistry*, John Wiley & Sons, Inc.

Wereley, S. T., and Lueptow, R. M. (1994). "Azimuthal velocity in supercritical circular Couette flow." *Experiments in Fluids*, **18**, 1-9.

Zeman, L. J., and Zydney, A. L. (1996). *Microfiltration and Ultrafiltration: Principles and Applications*, Marcel Dekker, Inc., New York.
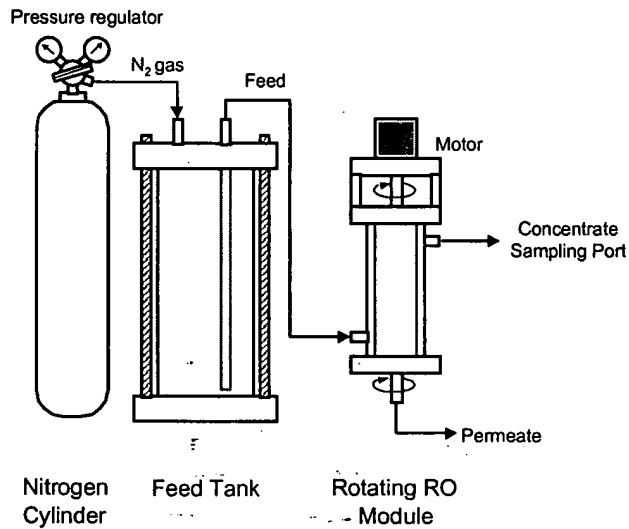
Figure 1. Schematic diagram of experimental flow circuit for rotating RO
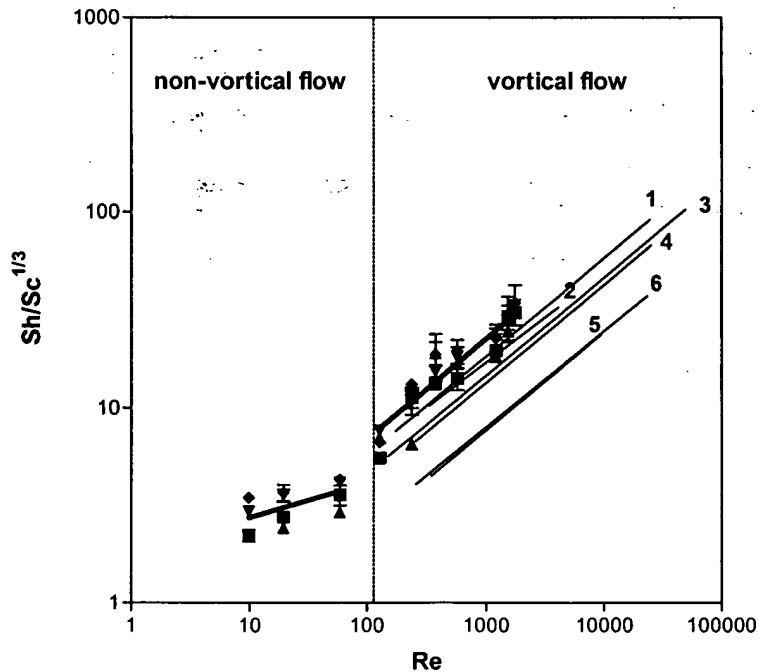
Figure 2. Mass transfer correlations in rotating RO. Filled symbols indicate the experimental data. Error bars are smaller than the symbol size except in cases where error bars are shown. Bold lines indicate a least squares fit. (■: NaCl, 6 atm; ▲: NaCl, 8 atm; ▼: NaCl, 10 atm; ◆: Na_2SO_4, 10 atm)

1. Holeschovsky and Cooney, 1991   2. Baier, 1999

3. Mizushina, 1971   4. Kawase and Ulbrecht, 1988

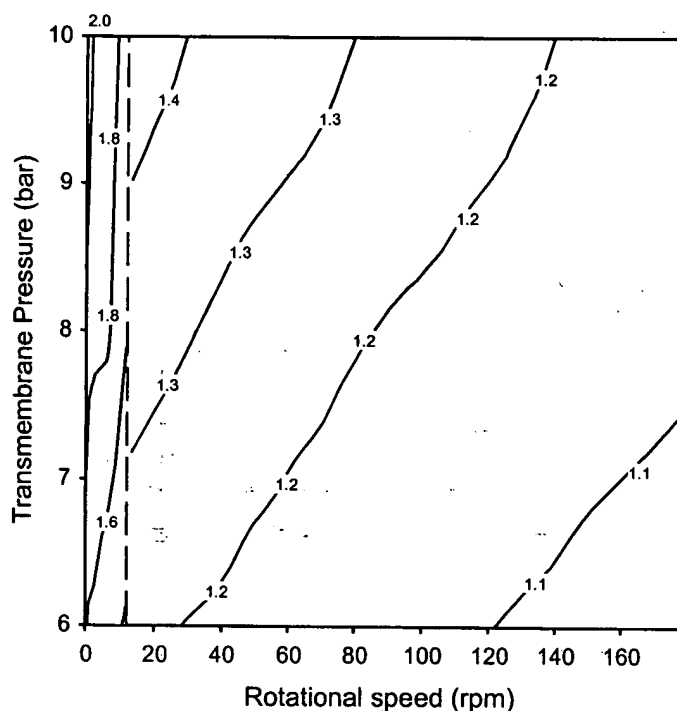5. Coeuret and Legrand, 1981   6. Kataoka et al., 1977

Figure 3. Contours of the concentration polarization ratio ($f=C_m/C_b$) for the case of NaCl 4000 mg/L solution at different transmembrane pressures and rotational speeds. The vertical dashed line represents the rotational speed for transition from non-vortical to vortical flow.